SUPERCONDUCTING FILTERS AND PASSIVE COMPONENTS

The advent of high-temperature superconducting (HTS) materials has enabled a number of applications in passive microwave electronics. Superconductors exhibit very low losses at microwave frequencies and, although finite, at the practical operating temperature of 77 K (boiling point of nitrogen), these losses are more than two orders of magnitude lower than normal conductors at frequencies of 10 GHz and below. This has allowed the possibility for high-performance planar microwave components since high-quality epitaxial films can be deposited on both sides of low microwave loss, single-crystal substrates allowing the fabrication of components in planar configurations such as microstrip, stripline, and coplanar waveguide. These configurations are widely used throughout the microwave community in a variety of technologies ranging from GaAs microwave monolithic integrated circuits (MMIC) to integrated circuits using ceramic and laminated substrates. Figure 1 shows a schematic cross-section of all three most common planar microwave structures. The use of HTS in these circuit configurations results in passive devices such as resonators, filters, and delay lines with performance far superior to conventional planar technology and with the attractive feature that many well-established design techniques can be used for HTS circuits as well.

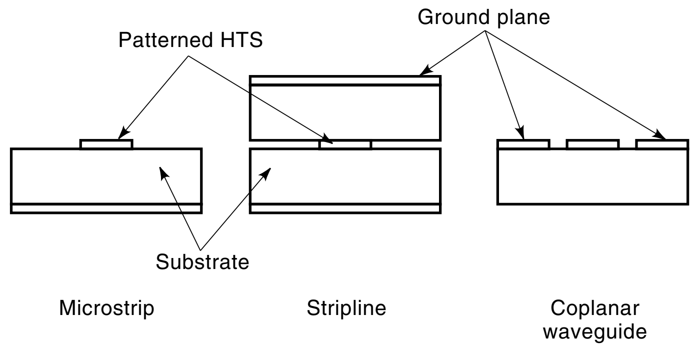

Figure 1. HTS technology lends itself to the fabrication of microwave planar devices such as those schematically depicted here in cross-section. One advantage of coplanar waveguide (and its variant slotline, not shown) is that only one patterned HTS film is needed. One disadvantage of stripline is that it is difficult to package. HTS devices have been demonstrated in all three structures.

The discussion in this article will focus on HTS microwave technology with the understanding that conventional low-temperature superconductors (LTS), for example, Nb or NbN, can also be used in the same fashion. Practical LTS materials operate typically at 4.2 K, the boiling temperature of liquid He. Furthermore, it should be kept in mind that a larger variety of substrates can be used in LTS technology because it does not require single-crystal epitaxial films. For example, Nb microwave and digital circuits have been demonstrated on Si and single-crystal sapphire (1).

HIGH-TEMPERATURE SUPERCONDUCTING FILM PROCESSING TECHNOLOGY

The basic elements of HTS thin-film technology from the point of view of microwave applications will be discussed here briefly. Only epitaxial thin films will be addressed because, to date, significantly better properties can be obtained from epitaxial material than from polycrystalline, nonepitaxial techniques. Most, if not all, of the developments covered in this article, however, are valid for the case of polycrystalline materials. The main advantage of these materials is cost and coating of nonplanar surfaces like the inside of a cylinder to form a high-Q cavity resonator (2).

Among the various high-temperature superconductors there are two that have achieved a level of maturity and acceptance in the industry: (1) $YBa_2Cu_3O_7$, usually referred to as YBCO, and (2) $Tl_2Ba_2CaCu_2O_8$ or TBCCO. High-quality epitaxial thin films of these materials can be deposited on both sides of a variety of low microwave loss, single-crystal substrates by physical vapor deposition techniques, mainly sputtering (3) and laser ablation (4) and also by metal-organic chemical vapor deposition (MOCVD) (5) and coevaporation (6). The two most common substrates to date are $LaAlO_3$ (LAO) and MgO. Circuits on sapphire have been demonstrated but the crystal lattice mismatch between HTS and sapphire is large enough to restrict the film thickness to below desirable values of at least 500 nm. Both LAO and MgO

Table 1. Basic Characteristics of the Most Used HTS Thin Films and Dielectric Substrates for Microwave Applications

HTS Films	YBCO	TBCCO
Critical Temperature (T_c)	90 K	105 K
Surface resistance (R_s) at 77 K and 10 GHz (f^2 dependence)	0.2–0.5 mΩ	0.2–0.5 mΩ
Film thickness	400–600 nm	800–1000 nm
Critical dc current density (J_o) at 77 K	10^6 A/cm^2	10^6 A/cm^2
Penetration depth (nm)	200 nm	200 nm
Substrates	**$LaAlO_3$ (LAO)**	**MgO**
Relative dielectric constant (ε_r) at 77 K	23.4	9.7
Dissipation factor (tan δ) at 77 K	$<10^{-5}$	$<10^{-5}$
Typical dimensions	5, 7.5, and 10 cm diameter; 250 and 500 μm thick	5 and 7.5 cm diameter; 250 and 500 μm thick

Both types of HTS Films can be grown in either substrate.

substrates are available commercially from a variety of suppliers around the world and can be readily obtained in circular wafers up to 7.6 cm in diameter and 250 μm to 500 μm in thickness. At 77 K and for frequencies between 1 GHz and 10 GHz the loss factor (tan δ) of LAO and MgO is less than 10^{-5}. This is 10 to 100 times smaller than most practical microwave substrates and is compatible with the low conductor loss of HTS.

YBCO is typically grown in situ as an epitaxial single-crystal film with thickness ranging from 400 nm to 600 nm. This means that the desired crystalline phase of the material is formed as the film grows because the growth conditions can be adjusted to obtain such results. In contrast, an amorphous film of TBCCO is deposited first and then the film is subjected to a postdeposition annealing treatment to form the right crystalline phase. One advantage of the in situ deposition of YBCO films is the ability to deposit other crystalline layers such as insulators or normal conductors, needed for the fabrication of Josephson junctions. HTS microwave technology can leverage the research on Josephson junctions by making use of insulating layers in other ways such as lumped element capacitors, for example. TBCCO films have the advantage of a higher critical temperature (Table 1) and are typically grown with thickness close to 1 μm. These are advantages because practical devices must be made with thicknesses two or three times greater than the London penetration depth (200 nm to 300 nm) at 77 K. TBCCO films thus offer a greater operating margin than YBCO films.

The most important characteristics or these two HTS materials and their substrates are given in Table 1. The properties listed are those a microwave designer would want to know if engaged in an HTS device design project.

Device Processing

Fabrication of microwave devices using either YBCO and TBCCO follows relatively straightforward photolithographic techniques. Patterning of the superconducting layer is typically accomplished by Ar-ion milling. The processing must include the deposition and patterning of low-resistivity contacts for interfacing with other devices or instrumentation. These are typically made by depositing a thin (200 nm to 300 nm) layer of gold or silver followed by an annealing step at 500°C to 600°C (7). Interfacing with other devices via coaxial connectors or directly to other substrates, superconducting or otherwise, can be accomplished using gold wire or ribbon attached to the low-resistivity contacts by ultrasonic thermal compression bonding or gap-welding (ribbons). Fabrication details of filters and delay lines made at Northrop Grumman can be found in (8). Other institutions follow similar procedures.

Microwave Packaging of High-Temperature Superconducting Devices

Proper packaging of cryogenic microwave devices is critical to the success of the technology. In general, planar microwave devices are made up of a dielectric or semiinsulating substrate, typically mounted on a metallic package or carrier by means of conducting epoxy or soldering. The mounted device then interfaces with other devices or measurement instrumentation most commonly via coaxial connections. In this case, the metallic carrier forms part of the ground terminal by connecting to both the outer jacket of the coaxial interconnection and the ground plane defined on the substrate. This means that microwave currents flow into the planar device through the center conductor of the coaxial interface and back out through the ground plane on the substrate, the metallic carrier, and its connection to the coaxial connector outer jacket. This current flow into the packaging assembly must occur without appreciable impedance mismatch or discontinuity. Figure 2 illustrates these points schematically with an example for a microstrip device.

The criticality of these connections between substrate, carrier, and connectors is exacerbated when cryogenic cooling of the microwave package is required because a large thermal mismatch between the various components may cause cracking of the substrate or degradation of the interface between substrate and carrier or connector. Furthermore, the quality of the interface between the cryoelectronic substrate and the outside world must be preserved through many temperature cycles between ambient and cryogenic temperature to allow for repeated testing of the device and an operational environ-

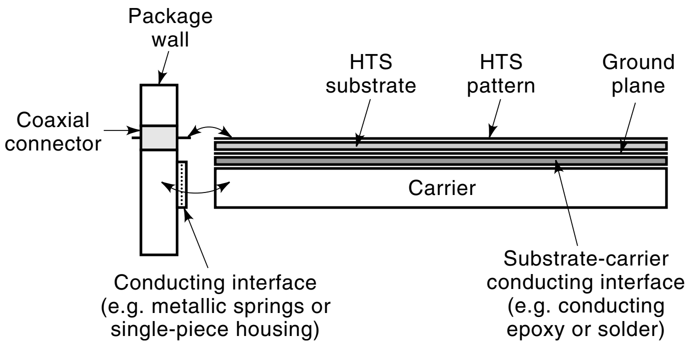

Figure 2. Microwave packaging of HTS devices is challenging because mechanical and electrical integrity must be maintained when the device is cycled from ambient to cryogenic temperatures. Special attention must be paid to the ground-current return path so as not to introduce parasitic reactances that could severely affect the performance.

ment, which may require that the device warm up to room temperature while not in use. Suitable microwave package designs must therefore include one or more of the following elements: (1) the use of thermally matched materials, (2) adhesives that remain sufficiently pliable at cryogenic temperatures, and (3) configurations that allow the various parts of the package to contract and expand freely while maintaining good electrical contact.

When considering materials that are thermally matched to HTS substrates the important parameter is the total contraction between room temperature and the operating temperature, for example, 77 K, and not the thermal coefficient of expansion. Figure 3 shows the relative thermal contraction for several materials, including LAO and MgO, in μm/cm (i.e., at a given temperature, a 1 cm-long piece of material shrinks so many μm from its length at 300 K). As can be seen, the slope of this curve, that is, the thermal coefficient of expansion, varies greatly with temperature over the range of interest, making it a practically useless parameter for the selection of appropriate materials. Although there are some differences in the rate of contraction as the materials shrink from room

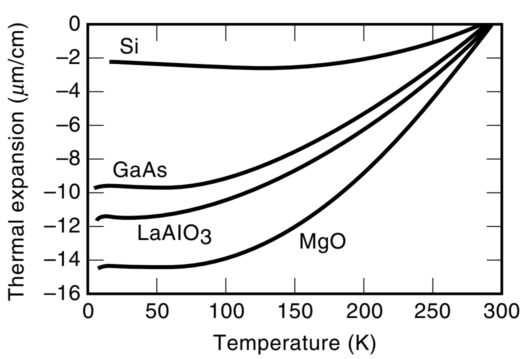

Figure 3. Measured relative thermal contraction of several materials of interest in HTS technology, including Si and GaAs. These or similar data should be used in the selection of carrier materials and the packaging of hybrid HTS-semiconductor components. If a good thermal match between parts that must remain in intimate mechanical and electrical contact cannot be obtained, sufficiently pliable conductive adhesives may be adequate for some applications, particularly if the mismatched parts are small.

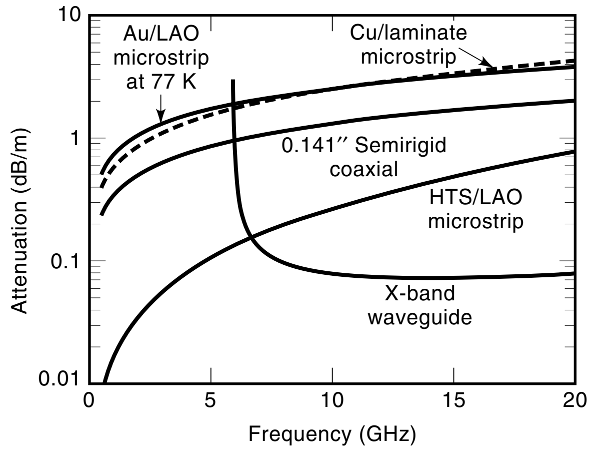

Figure 4. Calculated attenuation comparison for various transmission line types including HTS and gold microstrip on 500 μm-thick LAO substrates. The line impedance for each line was 50 Ω. All microstrip substrates were assumed to be 500 μm thick. Notice that X-band waveguide has lower loss than HTS microstrip (for the parameters chosen). However, HTS microstrip has broader bandwidth and the potential for smaller volume because it facilitates the integration of several microwave components.

temperature, the key parameter is the total contraction at 77 K. For example, Nb and LAO are fairly well matched at 77 K, even though their rate of contraction as a function of temperature is slightly different. This is borne out by extensive experimentation (8). Other substrate/carrier material pairs have been successfully used as well.

PASSIVE SUPERCONDUCTING MICROWAVE DEVICE FUNDAMENTALS

The key reason for developing a microwave HTS technology is the exploitation of the low loss afforded by HTS compared with conventional metals like gold and copper. High-performance, low-loss devices using conventional materials can generally be made at the expense of high volume, usually in the form of hollow or partially dielectric-filled waveguide components. The potential of HTS is to enable components with the same or better performance in a much reduced volume which must include the cryocooler. Figure 4 shows a comparison between calculated losses in several common types of transmission line, including HTS microstrip on LAO, for the parameters listed in Table 1. For calibration, included in this comparison is Au microstrip at 77 K, also on LAO. For the microstrip cases only the conductor and dielectric losses were calculated; radiation losses or coupling to spurious surface modes were ignored. Also included are the losses in X-Band waveguide, which are lower than HTS for the parameters chosen, although HTS microstrip offers the advantage of much wider bandwidth and ready integration of several components into a small volume. Notice that the useful frequency range for X-band waveguide is typically only 8 GHz to 12 GHz. Integration capability combined with low loss are key elements of HTS technology because most systems insertion opportunities will arise for applications offering significant size advantages with respect to conventional approaches.

A different and also useful way of getting insight into the advantages of HTS planar circuits is from the point of view of resonant structures, which form the basic building block of passband filters. This can best be discussed in terms of quality factor, Q, which is the ratio between stored and dissipated energy:

$$Q = \frac{\text{Stored energy}}{\text{Dissipated energy}} \tag{1}$$

For empty electromagnetic cavity-type resonators, this is, in essence, a figure of merit measuring the degree of compromise between volume (stored energy) and surface area (microwave losses on the conducting surfaces). In general, both stored and dissipated energy depend on the dielectric constant and the geometric configuration used, the dissipated energy depending also on the surface resistance of the (super)conducting surfaces and the losses in the dielectric. In practice, there could be other types of losses such as radiation, which, for simplicity, will be neglected in this discussion. In principle, the performance of any passive device can be projected from the Q of the type of structure used to make up the device. For example, a resonator made up of a section of microstrip line can be calculated from well-known expressions (9). The insertion loss of a filter can, in turn, be estimated from the Q of the resonators that make up the filter (10).

Figure 5 is a plot comparing the Q and volume, as a function of frequency, of resonators made up of a microstrip line section and an empty metallic cube, respectively. Since the dimensions of the resonator are specified at each frequency, the volume calculated is that of the smallest cube capable of resonating at a given frequency. The microstrip HTS resonator volume was calculated assuming it is in an enclosure with cross-section as shown in the figure, where the walls and the lid are sufficiently far away from the superconducting strip that their contribution to the loss is negligible. The Q of HTS microstrip, although higher, is within the same order of magnitude as the Q of the cube resonator. However, the estimated volume can be two or more orders of magnitude smaller, especially at the lower microwave frequencies.

Although to first order the main feature distinguishing HTS from conventional planar microwave passive devices is low loss, other important differences exist and are discussed in the following sections.

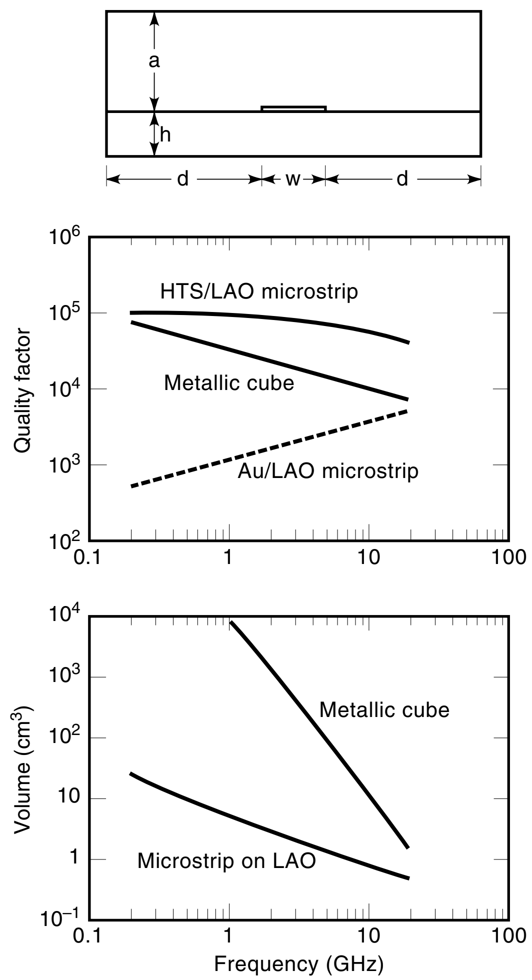

Figure 5. Calculated comparison of quality factor (Q) and volume for two types of resonators: 50 Ω HTS microstrip on 500 μm-thick LAO and a metallic cube. The Q of a gold-on-LAO microstrip at 77 K was also calculated as a reference. The metallic cube is representative of a simple cavity resonator and was chosen because its Q is easy to calculate (12). The volume for the microstrip was chosen as a device with the cross-section shown in the figure with $a/h = 10$, $d/h = 20$, and a length of $(\lambda/2 + 4h)$. This assumed cross section is independent of wavelength and loses its meaning at the higher frequencies plotted, where the substrate would, in practice, be thinner, making the microstrip always smaller than the waveguide.

Surface Impedance and Penetration Depth

The surface or internal impedance of a conductor is the characteristic impedance seen by a plane wave incident perpendicularly upon a planar (super)conducting surface. For both normal (e.g., copper, gold) conductors and superconductors, the surface impedance per unit length and width is given by (11,12):

$$Z_S = R_S + jX_S = \sqrt{\frac{j\omega\mu}{\sigma}} \tag{2}$$

where ω is the angular frequency, μ is the permeability, and σ is the conductivity. σ is real for normal conductors but is complex for superconductors. In both cases the RF fields decay exponentially inside the material, defining a field penetration depth. In the case of superconductors, however, this parameter is independent of frequency and is orders of magnitude smaller than the normal conductor penetration depth (usually referred to as the skin depth). The reasons are derived from the perfect diamagnetism of superconductors, the so-called Meissner effect, and are explained by the Gorter-Casimir and London two-fluid model of superconductivity (11,13).

Table 2 summarizes the differences between normal and superconductors from the point of view of their microwave surface impedance. Notice that the surface resistance of superconductors, R_s, has a frequency-squared (f^2) dependence. In contrast, normal conductors depend on the square root of frequency ($\sqrt{f}$). Figure 6 shows the difference between copper at 300 K and 77 K, and HTS at 77 K. This must be taken into consideration, especially when designing wide-band compo-

Table 2. Microwave Surface Impedance Comparison Between Normal Conductors and Superconductors

$$Z_S = R_S + jX_S = \sqrt{\frac{j\omega\mu}{\sigma}}$$

Normal Conductors	Superconductors
σ = Real	σ = Complex
Penetration (skin) depth: $\delta = \sqrt{\frac{1}{\pi f \mu \sigma}}$	Penetration depth: $\lambda_L(T) = \frac{\lambda_L(0)}{\sqrt{1-\left(\frac{T}{T_C}\right)^2}}$ $\lambda_L(0) \cong 150$ nm for YBCO
$R_S = X_S = \frac{1}{\sigma\delta} \propto \sqrt{f}$	$R_S \propto f^2$ $X_S \cong 2\pi f \mu \lambda_L$
Copper at 300 K: $\delta = \frac{2.1}{\sqrt{f}}\,\mu$m $R_S = 8.24\sqrt{f}\,$mΩ	YBCO at 77 K: $\lambda_L(77) \cong 0.2\ \mu$m $R_S = 5f^2\ \mu\Omega$
Copper at 77 K: $\delta = \frac{0.9}{\sqrt{f}}\,\mu$m $R_S = 3.4\sqrt{f}\,$mΩ	

nents. The figure also highlights the large difference between copper and HTS at frequencies below 1 GHz.

As with planar microwave devices using normal conductors, best performance control is obtained when the geometric inductance of the circuit dominates the kinetic (or internal) inductance of the superconductor. That is, from a practical point of view, the thickness of the superconductor must be at least two to three times larger than the penetration depth at the temperature of operation. The penetration depth is a strong function of temperature and for HTS it is given approximately by (11,13).

$$\lambda_L(T) = \frac{\lambda_L(0)}{\sqrt{1-\left(\frac{T}{T_C}\right)^4}} \tag{3}$$

where $\lambda_L(0)$, the penetration depth at 0 K, is a fundamental parameter of the material, T is the temperature and T_c is the

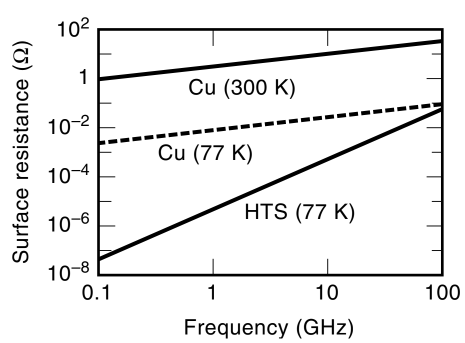

Figure 6. Surface resistance of HTS at 77 K and copper at 77 K and 300 K as a function of frequency. The surface resistance of copper scales with frequency as $f^{1/2}$; for HTS it scales as f^2.

critical temperature. For YBCO, $\lambda_L(0) \cong 150$ nm, which results in $\lambda_L(77\ \text{K}) \cong 214$ nm. The HTS film must be at least 500 nm to 600 nm thick for operation at 77 K, in order for the kinetic inductance effects to be negligible with respect to the total inductance of the circuit.

For practical microwave design purposes, this allows treating the superconductor as a normal conductor with a surface resistance that can be obtained from measured values and a frequency-squared scale factor. It has become customary for workers in the field to normalize the surface resistance to 10 GHz and 77 K, even though measured data may have been taken at a different frequency. Devices where the kinetic inductance is allowed to dominate have been demonstrated (14). However, they are lossy, difficult to fabricate, and quite dependent on temperature because of the strong temperature dependence of the penetration depth.

$LaAlO_3$ (LAO) Substrate Properties

The relative dielectric constant of LAO, one of the preferred HTS substrates, is $\epsilon_r = 23.4$ at 77 K. This is a higher value than most common microwave substrates whose dielectric constants usually do not exceed 10 ($\epsilon_r = 9.7$ for MgO, another preferred HTS microwave substrate). The significance of this is that common planar component design techniques are based on empirical circuit models whose validity may not extend to the relatively high dielectric constant of LAO. For example, the design of microstrip parallel-coupled-line filters involves the use of quarter-wave coupled-section models that generally are not valid for $\epsilon_r > 18$. This requires that more sophisticated design techniques be developed, making use of electromagnetic field solvers, for example, or empirically extending the range of existing models.

LAO has a cubic crystal structure above about 450°C. Below that temperature it transitions to a rhombohedral structure, which is only a slight distortion from the cubic structure consisting of a very small stretching of the cubic unit cell along its diagonal. In order to release stress, the crystal will form twin structures, symmetrically related regions oriented in different directions. Noncubic crystals are anisotropic and, as a result of this twinning, the LAO substrate is made up of slightly anisotropic regions randomly distributed throughout the substrate (11). The net result is an average dielectric constant with a uniformity of approximately 1%. This means a 2% variation in the resonant frequency of a planar resonator and there are many filter applications, for example, where this is not acceptable. In contrast, MgO, which is cubic, has a uniformity of 0.1% (15).

Dynamic Range Considerations: Noise Figure

An important consideration for any electronic device is its dynamic range, or range of signal power levels over which the device will operate properly. In the case of passive HTS devices, they are expected to be linear over a certain dynamic range, limited below by noise and above by the onset of nonlinear behavior.

Starting at the lower end, the noise generated in a passive device will generally be of a thermal nature. A measure of how much noise any device generates is given by the noise figure (16), which is, by definition, related to the excess noise generated in the device when a matched resistor at 290 K (ambient temperature) is placed at the input. Thus the noise figure would be equal to 1 (or, equivalently, 0 dB) if the device were perfectly noiseless or if it were an ideally lossless passive device. The accepted noise figure definition as a function of device temperature is (16).

$$F_{\mathrm{dB}} = 10 \cdot \log\left[1 + (L-1)\cdot\frac{T}{290}\right] \tag{4}$$

Here, L is the insertion loss of the device as a number greater than or equal to 1 (i.e., $10\log(L) \geq 0$ dB) and T is the temperature in degrees Kelvin. For a passive, lossy device at 290 K, the noise figure turns out to be equal to its insertion loss, a rule that system designers commonly use when dealing with passive components such as filters or lengths of transmission line. HTS devices, however, because they operate at cryogenic temperatures (77 K, typically), will have a lower noise figure, according to the accepted definition (16). Figure 7 shows this expression graphically as a function of the insertion loss of the device for 77 K and 290 K (ambient temperature). Thus, in considering the dynamic range of HTS devices, the lower end of the range will tend to be lower than for conventional devices, not only because of their inherent low loss, but also because they operate at cryogenic temperatures. Measurements reported in the literature (17) confirm, to first order at least, that the noise in HTS passive devices is indeed thermal in nature.

Dynamic Range Considerations: Nonlinearity and Power Handling

The dynamic range of HTS passive devices is limited above by nonlinearities in the superconductor. This is in contrast to conventional technology, for which this upper limit could be orders of magnitude higher, generally limited by such phenomena as the voltage breakdown of air or the dielectric used, or melting of the metallic pattern due to high currents. HTS, on the other hand, is fundamentally limited by the critical magnetic field, above which the material loses its superconducting properties. Nonlinear behavior occurs as the RF magnetic field approaches its critical value. Furthermore, in practical devices the microwave fields will generally tend to be nonuniformly distributed so that critical values are exceeded first in selected areas of the device. For example, a microstrip line has much higher current density near the edges of the line than along the center. Thus, as the signal power level is increased, the current density at the line edges will approach critical state first, generating nonlinearities and increased losses, degrading the performance of the device.

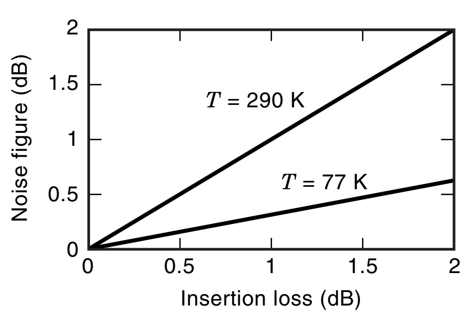

Figure 7. Noise figure of a cryogenically cooled passive device as a function of insertion loss. Notice that the noise figure equals the loss at 290 K (by definition), but it is lower for devices operating at a lower temperature.

When a device is nonlinear it produces intermodulation distortion; that is, two signals of different frequencies applied to the device will generate mixing products. In general, the largest mixing products are those of the third order. The upper end of the dynamic range is then reached when the power level of the applied signals is such that the third-order products rise above the noise floor and can be mistaken and processed by the system as real signals. The nonlinear behavior in a device is characterized by the third-order intercept point (TOI) (18).

A system dynamic range can, in turn, be determined from that of its components. An important example is that of a microwave receiver front-end, usually consisting of a low-noise amplifier (LNA) placed after the antenna, which is then followed by one or more downconversion stages. The dynamic range of the receiver is greatly determined by the noise figure, gain, and TOI of the LNA, with the components that follow having much less influence. Many applications demand a preselector filter between the antenna and the LNA to reject strong interfering signals that could generate unwanted mixing products due to the nonlinearity of the LNA (17). The preselector filter must not significantly degrade the receiver dynamic range and so it must have low insertion loss (i.e., low noise figure) and a TOI sufficiently higher than the LNA's with respect to both in-band signals and the rejected out-of-band interfering signals. This is an important example because HTS filter technology is a strong candidate for this type of preselector in some applications like wireless communications base-station receivers (19).

The linearity condition, which may be a relatively minor issue with conventional filter technology is, in contrast, very key in HTS filter technology. Specific developments in this area will be discussed in the section on HTS Filter Technology.

A fundamental characterization of the nonlinear behavior and power handling in HTS materials is through the surface impedance and its dependence on the RF magnetic field H_{RF} (20–25).

$$Z_s(H_{\mathrm{RF}}) = R_s(H_{\mathrm{RF}}) + jX_S(H_{\mathrm{RF}}) \tag{5}$$

The essence of the nonlinear dependence of the surface impedance on signal power level or, equivalently, H_{RF} is readily understood by observing the response of a microstrip resonator, shown in Figure 8. As the input power is increased the resonator Q degrades (R_s dependence on H_{RF}) and the resonance shifts to lower frequencies (X_s dependence on H_{RF}). Several regimes have been identified in the study of nonlinear phenomena in HTS (22). A linear region at sufficiently low power levels, a weakly nonlinear region where nonlinear behavior is dominated by grain-boundary weak links (Josephson-junction-like defects in the crystalline make-up of the HTS film) and a strongly nonlinear region dominated by hysteretic vortex penetration. Above this regime breakdown of the superconducting state occurs, with the surface resistance increasing abruptly due to heating and the formation of normal-state domains (22).

If the magnetic field exceeds its critical value the material becomes a normal conductor and dissipates heat which must be removed by the cryocooling system and can even damage

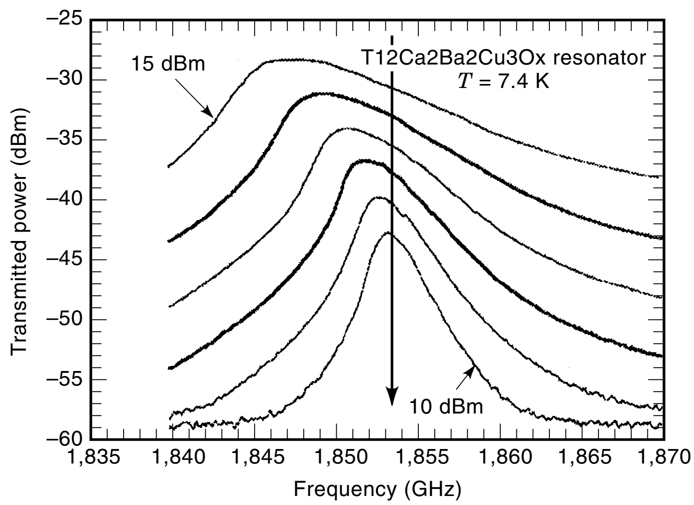

Figure 8. Effect of increasing the input power level on a superconducting microstrip resonator. This measurement (courtesy of Dr. M. Golosovsky, Hebrew University of Jerusalem) captures the essence of the nonlinear RF power dependence of the surface impedance $Z_s = R_s + jX_s$. As power level increases so does R_s and the resonance Q decreases. On the other hand, the effect of increased power level on X_s manifests itself on a shift of the resonance toward lower frequencies (22).

the device. The device ceases to operate as a superconducting device and, if no damage has occurred, must recover after the high-power source has been removed. The related topic of intentionally provoking a superconducting-to-normal transition as a switching mechanism has been studied extensively (26–28).

Systematic studies of intermodulation distortion in HTS samples and devices have been reported in the literature (21,29–32). TOI values in excess of +70 dBm at 1.3 GHz and 80 K have been obtained (29) for HTS planar transmission lines a few millimeters long. This is well above most semiconductor low-noise amplifiers, for example. However, it must be kept in mind that intermodulation distortion is a function of the stored energy in the device, that is, the group delay. This is important when considering the performance of HTS passband filters because filters have a delay characteristic that is lower near the center of the passband and higher toward the edges, depending on the filter order and type of response. Thus, in a practical situation, if a passband filter is intended to protect the system from a relatively high-power interfering signal, this signal may lay on the filter skirts at a given rejection level in a region of relatively high delay. The intermodulation of this interferer with a desired signal in the middle of the passband (relatively low delay) will produce spurs that define the dynamic range of the filter from that specific system's perspective. To give a quantitative example, such dynamic range might be specified as a third-order intermodulation spur level of −90 dBm for an interfering signal of +40 dBm maximum power at ± 15 MHz from a desired signal at passband center that has a maximum power level of +5 dBm. In a case like this it would be difficult to talk about TOI, which is usually defined as resulting from the intermodulation of two signals of the same power level. Such a definition would apply to a spur-free dynamic range specification for the straightforward case of two in-band signals undergoing the same group delay.

HIGH-TEMPERATURE SUPERCONDUCTING FILTERS

One of the most important applications of HTS microwave technology are high-performance passband filters because they can be made in planar configurations. Filters are often the dominant contributor to system volume, in particular when banks of low-loss filters are required. As discussed earlier, high-Q structures can be obtained at the expense of high volume. HTS planar configurations like microstrip or coplanar waveguide have Q comparable to cavities at a much smaller volume (see Fig. 5) and so HTS is an attractive approach to reducing the volume of high-performance filters.

A straightforward way of thinking of bandpass filters is as coupled resonators. The performance of a resonator is characterized by its quality factor Q, defined in Eq. (1). When the resonator forms part of an electrical circuit, the circuit delivers and takes back energy from the resonator, affecting its characteristics. The unloaded Q of a resonator, Q_u, is its intrinsic quality factor, without the effects of an external circuit. A first-order filter consists of a single resonator. Its bandwidth can be adjusted by the degree of coupling into the resonator by the external circuit. In a lightly coupled resonator, little disturbance is introduced by the input and output circuits and its resonant conditions and bandwidth are close to those of an ideal, unloaded resonator. When coupling into the resonator is strong, the disturbance is large and the Q is now dominated by both the resonator and the external circuit, making the total or loaded Q lower than the ideal, unloaded Q, and therefore the filter bandwidth is now wider. For a higher-order filter made up of various resonators coupled together, the idea is the same. Narrow-band filters require that the resonators be loosely coupled to each other and the minimum bandwidth is limited by the unloaded Q of the resonators. Wider bandwidth filters will have tighter coupling among resonators. Clearly, then, narrow-band filters are a desirable application for HTS because its inherent high Q enables narrow bandpass filters with low loss and small volume. This was illustrated in Fig. 5, which helps to understand the significance of the loss–volume trade-off from the point of view of using HTS and metallic cavity resonators to make filters. There is also a trade off between bandwidth, filter order (number of resonators), and insertion loss. The following is an approximate expression for the mid-band insertion loss of a filter (10), in dB, which reflects this trade-off:

$$L_{\mathrm{dB},n} \cong \frac{4.34}{B} \cdot \sum_{k=1}^{n} \frac{g_k}{Q_{\mathrm{u}k}} \tag{6}$$

Here, n is the filter order, g_k are the normalized series inductance and shunt capacitance values of the low-pass prototype filter (10), B is the filter bandwidth as a fraction of the center frequency, and Q_{uk} is the unloaded Q of the kth resonator. For the purposes of estimation, it is reasonable to assume that all the resonators in the filter will have the same Q_u. Figure 9 illustrates the trade-off between insertion loss, bandwidth, and filter order as a function of resonator Q_u. It shows how expression (6) can be used to estimate the potential of a certain filter technology, in this case HTS, and understand its

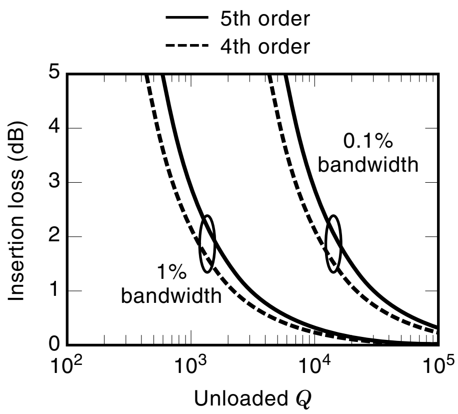

Figure 9. Estimated insertion loss of fourth- and fifth-order Chebychev passband filters of 1% and 0.1% fractional bandwidths as a function of the unloaded Q of the resonators that make up the filter. It was assumed that all the resonators have the same Q. The chart shows the increase in insertion loss caused by increasing the filter order by one and by reducing the fractional bandwidth by a factor of ten.

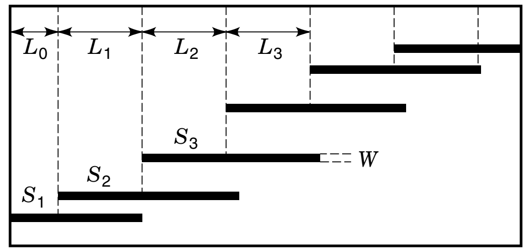

Figure 10. Parallel coupled microstrip or stripline filter topology. The lines are $\lambda/2$ resonators coupled as $\lambda/4$ backward-coupled sections. This is a well-known configuration suitable for fractional bandwidths of less than 15%; early demonstrations of HTS filters made use of it. However, control of the weak coupling required for bandwidths less than 1%, which the low loss of HTS allows, is very difficult and results in designs that are very sensitive to material and geometrical tolerances.

limitations. The insertion loss was estimated for Chebychev-type filters (10) of the fourth and fifth orders, respectively, and for 1% and 0.1% fractional bandwidths. The purpose of this chart is to point out the difference in loss caused by increasing the filter order by one and by increasing the fractional bandwidth by a factor of ten. Figure 9 complements Fig. 5 by helping to make a connection between the insertion loss of a filter of a given order and bandwidth and a specific structure and its volume. The information provided by these two figures can readily be extended to cover other structures and technologies.

Design Considerations

As discussed above, some of the most important applications of superconductors are in narrow passband filters because they can be realized in planar technology, which lends itself to small structures that can be readily integrated with other filters and circuitry. It was also discussed that the coupling between the resonators that make up a narrow-band filter needs to be weak. The mechanism for implementing weak coupling between resonators must allow for its control and predictability so that robust filter designs which are relatively intolerant of external spurious coupling mechanisms can be implemented. An example illustrating this point can be found in the parallel-coupled line filter topology. Figure 10 shows this topology, which is well known as being suited for microstrip filters with relative bandwidths below 15% (10). An analysis based on Figs. 5 and 9, however, shows that if HTS is used then bandwidths below 1% are possible from the loss standpoint. Indeed, this structure was used by several research groups to make initial HTS filter demonstrations with 1% to 2% fractional bandwidths (33,34). Table 3 shows the couplings required to achieve a 1.25% bandwidth, fourth-order Chebychev filter with 0.1 dB ripple at 4 GHz (8), as well as the distance between resonators (see Fig. 10). This distance was calculated using commercial software based on coupled microstrip line circuit models and a simple look-up table technique (8) generated using a two-dimensional electromagnetic field solver as a tool to refine the results of the circuit-model-based software. The effectiveness of this technique was demonstrated experimentally (8). Notice in Table 3 that two of the three required couplings are less than −30 dB and that the error in estimating the coupled-line distances given by the circuit-model software increases as the coupling gets weaker. For narrower bandwidths, weaker couplings are needed, which would result in larger separation between resonators and hence increased difficulty in accurately predicting and controlling the required coupling. Bandwidths of less than 1% with this filter topology could probably be achieved with great difficulty and very low yield because of the practical issues associated with controlling the weak couplings required (35).

Workers in this field have realized this fundamental problem and have identified structures which allow significantly better control of weak interresonator coupling. Recognizing that in microstrip backward-coupled resonators, such as those in Fig. 10, the problem is compounded by the presence of spurious forward coupling, researchers have demonstrated good coupling control using forward-coupling alone in microstrip (36) and backward coupling alone in stripline (37). Also, the use of planar lumped elements (38), and inductive coupling in coplanar line (39,40) have been demonstrated successfully. Today, HTS filters are being made with bandwidths of 1% or less by dedicated commercial companies for the base-station wireless market as preproduction prototypes (19,41).

Complex Structures

The potential for filters with performance similar to bulkier waveguide components but at significantly smaller sizes can be most readily fulfilled for the case of banks of filters,

Table 3. Comparison Between Conventional and Look-Up Table Approaches (see Fig. 10)

Parameter	Required Coupling (dB)	Conventional (mm)	Look-Up Table (mm)
S_1	−17.6	0.572	0.530
S_2	−35.8	2.367	1.931
S_3	−37.8	2.772	2.161

f_o = 4 GHz; W = 0.176 mm; $L_1 \cong L_2 \cong L_3 \cong$ 4.788 mm.

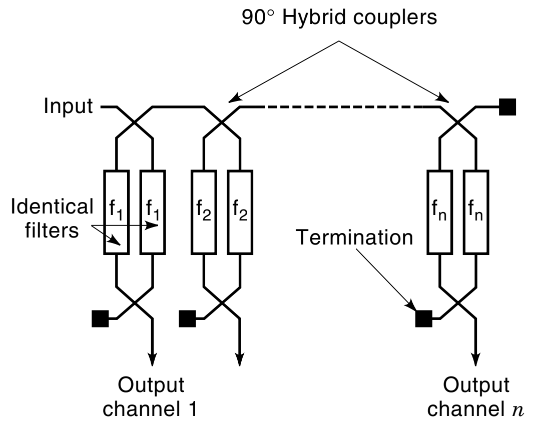

Figure 11. Multiplexer architecture used to demonstrate a four-channel HTS microstrip device. This configuration has the advantage of allowing as many channels as the bandwidth covered by the 90° hybrid. Each filter is terminated in 50 Ω and is essentially isolated from the others. Other schemes require that the impedance termination in each filter be adjusted to account for the presence of all the filters in the multiplexer, practically limiting the maximum number of channels to ten or twelve.

whether switched or multiplexed. Because HTS technology is planar, a relatively high level of integration is possible so that, as opposed to waveguide or dielectric resonator filter technology, a bank of N filters each occupying a volume V occupies a volume $< N \times V$, where V is significantly smaller than for conventional technologies for the same performance. HTS filter banks have been demonstrated by several groups in the form of bandpass multiplexers (8,42–44) or banks of switched band-reject filters (45).

Example: Four-Channel Pass-Band Multiplexer. Figure 11 shows a diagram of a multiplexer architecture (8,42). It can accommodate as many channels as the bandwidth of the 90° hybrid coupler covers. Input microwave energy is equally split at the first coupler. If the frequency is within the passband of the two identical filters connected to the coupler, it passes through the filters and adds in phase at the output port of the output hybrid coupler for Channel 1. If the frequency is not within the passband of the Channel 1 filters, the signal is reflected back to the input coupler where it recombines such that it is out-of-phase at the input port and in-phase at the input of the second channel hybrid coupler. The process then repeats itself until the signal exits the device through the appropriate channel port. Figure 12 presents details of one implementation of this device (8,46) showing one input, four outputs, and a through port terminated in an external (coaxial) load. Additional channels could be connected to this port provided they are still within the bandwidth (about 10%) of the hybrid coupler used in this demonstration. Figure 12 also shows a detail of the assembly, which includes the internal HTS interconnections between filters and the integrated thin-film resistive terminations at the out-of-phase port of the output hybrid in each channel.

The HTS material used for this work was YBCO thin film deposited on 500 μm-thick LAO substrates. The package included an aluminum frame holding the external coaxial connectors and niobium carriers onto which the LAO substrate pieces were mounted. Niobium is a good thermal expansion

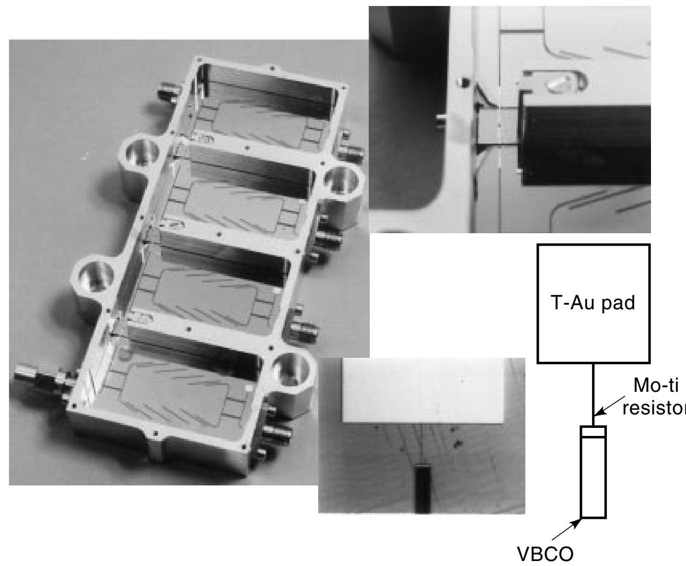

Figure 12. Photo montage of a four-channel YBCO-on-LAO microstrip multiplexer demonstrated under the US Navy's High-Temperature Superconductivity Space Experiment II (HTSSE-II). Details of the design, fabrication, and assembly of this device can be found in Refs. 8 and 46.

match to LAO, so the electrical and mechanical integrity of the device was preserved when cycling from ambient temperature to near 77 K. The substrate-carrier assemblies were mounted on the aluminum frame using a beryllium-copper spring arrangement. Figure 13 shows the measured performance. The low-frequency skirts of Channels 2, 3, and 4 show some level of interaction between channels that can be eliminated using a wider guard-band between channels. Refs. 8 and 46 include a full discussion of the design, fabrication, and measurements on this device.

This unit was one of a series of demonstration devices delivered to the US Navy's High-Temperature Superconductivity Experiment II program by several contractors for inclusion into the space package (47).

High-Power-Handling Designs

The promising applications of HTS require that HTS filters handle sufficient signal power levels as to maintain linearity over a significant dynamic range. As explained earlier, current crowding along the edges of typical planar transmission

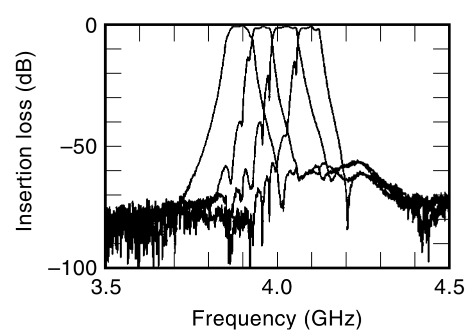

Figure 13. Measured response of the four-channel HTS multiplexer. Further details can be found in Refs. 8 and 46.

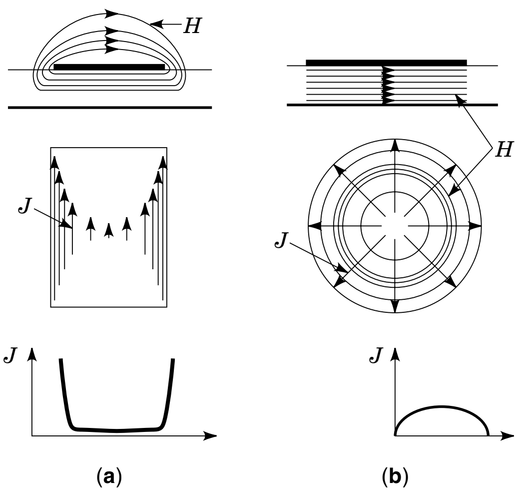

Figure 14. Diagram (courtesy of Dr. Z-Y Shen, E. I. du Pont de Nemours and Co.) (29), showing the magnetic field and current distribution in a $\lambda/2$ microstrip resonator (a) and a TM_{010} printed disk resonator (b). In the disk the magnetic field lines are circular and remain on the plane of the disk, so the current is not highly nonuniform as is the case of the regular microstrip resonator. The advantage of the disk is that it can handle much higher power levels (29,49,50).

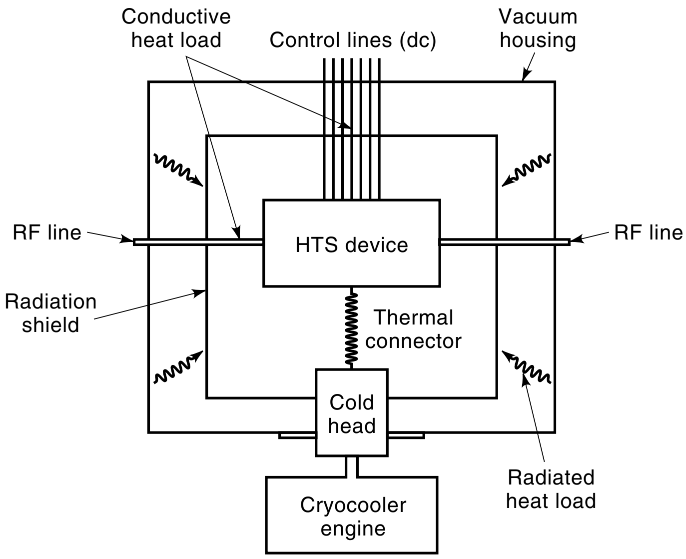

Figure 15. Schematic diagram of the cryogenic package for a hypothetical HTS device showing conducted heat inputs through input/output RF and dc control lines and the mechanical support of the cold head, as well as the radiated heat input from the (warm) wall of the vacuum housing. The purpose of this diagram is to show the main elements that affect the design of the cryogenic package.

lines (e.g., microstrip, stripline, and coplanar waveguide) ultimately limits the maximum power level that can be handled. Increasing the quality of the material and improving the design of filter structures has been a major endeavor at several institutions. Improved filter designs are based on planar structures which avoid the effects of significant current crowding at the edges, as is the case of low-impedance microstrip lines (48). Most significant is the work employing planar resonator structures based on the circular TM_{010} mode (29,49,50). The most salient features of this approach are shown in Figs. 14(a) and (b), which show the electromagnetic fields and current profile in a microstrip and a disk resonator, respectively. In the latter the RF magnetic fields do not close above the substrate but within it, under the disk. Thus the current density does not peak at the edges of the resonator and its distribution is more uniform. The only possible drawback of this approach is that the fields are more confined to the disk resonator, and intercoupling between resonators to form a filter may be more difficult, perhaps requiring three-dimensional structures for proper control of the coupling. This would eliminate some of the planar integration advantages. Fully planar filters using this concept, however, have been successfully demonstrated (29).

HIGH-TEMPERATURE SUPERCONDUCTING DELAY LINES

Work on superconducting delay lines started at Lincoln Laboratory well before the advent of high-temperature superconductivity, and concentrated mostly on linearly dispersive delay lines for analog signal processing. Linearly dispersive delay lines have delay characteristics which vary linearly with frequency over a certain operating bandwidth and can be used to perform pulse compression, a technique to process and detect small signals which may be below the receiver noise floor (1). The pioneering work at Lincoln Laboratory in this area using LTS and, more recently, HTS thin-film technologies has been extensively documented in the literature (1,51).

Table 4. Sample System Requirements That Will Affect the Choice of Cooler and Cryogenic Packaging Approach

Requirement	Comments
Size and weight	Stringent in almost all applications
Cool-down time	Some applications may require very fast turn-on time (e.g., a few minutes). They would be a driver toward higher cooler power and lower HTS device thermal mass
Vibration	For example, a minute amount of mechanical distortion on a circuit caused by vibration from the cooler may generate a phase modulation that degrades the circuit performance
Power consumption and power supply type	E.g., 120 V ac
Mode of operation	E.g., continuous, intermittent, short missions and then mostly idle, etc.
Temperature stability and control	While any fine temperature feedback control loop ($<\pm 0.01$ K) tends to be done using heaters and a temperature sensor, some applications may require a certain degree of cooling engine control ($<\pm 0.5$ K)
Unattended lifetime	Some applications (e.g., space) may require a lifetime on the order of 10 years or more
Vacuum lifetime	All-welded construction; use of getters in a clean, well-conditioned (baked) system

Table 5. Cooling Requirements That Will Influence the Cooling Power (Heat Lift) Required for a Given Application

Requirement	Comments
Power dissipated in the device	A filter with a 0.5 dB insertion loss that must pass a 20 W signal will dissipate 2 W of heat that must be removed by the cryocooler. Also, semiconductor devices such as low-noise amplifiers, which improve in noise and gain performance when cooled, always dissipate a certain amount of heat which must be taken into consideration
Number of microwave and dc control leads	These are the electrical interface between the cryocooled device and the outside world. For example, a filter might require two microwave leads (input and output) and two pairs of dc control lines for the heat sensor and a small heater to keep the temperature constant. These conductors represent a heat loss that the cooler must overcome because they connect the outside ambient temperature with the cold device. While the dc control lines are typically made of thin low-thermal-conductivity, high-resistivity wire (e.g., gauge 32 manganin), the microwave leads must achieve a compromise between insertion and thermal loss
Surface area	Radiation loss is another form of heat loss that the cooler must overcome and therefore must be minimized. The total surface area and their infrared radiation emmisivity are important design parameters. Low-emmisivity radiation shields are typically used between the warm vacuum vessel wall and the cold device
Thermal mass	For those applications that have a cool-down time requirement, the thermal mass of the device to be cooled is important and will be affected by the microwave packaging material and its shape

Nondispersive delay lines have a constant delay-versus-frequency characteristic and are typically used as analog memory elements that can store a signal for, say, up to a few hundred nanoseconds while the system is engaged in other processing steps. Work on HTS nondispersive delay lines has also been significant (52–55). Including two recent instantaneous frequency measurement subsystems based on banks of delay lines (52,55). Clearly, the advantages of superconductivity are that a long length of line can be fabricated in a small volume by defining a long, planar transmission line on a wafer. Ref. 54 compares conventional nondispersive delay lines, which require amplifiers between sections of transmission line (e.g., coaxial), with HTS delay lines using projections based on measurements made on relatively short (22 ns) delay lines. Key delay-line parameters are delay, bandwidth, insertion loss, and third-order intercept point. Conventional delay lines that must resort to amplification to boost the signal are limited in dynamic range by the amplifiers.

CRYOGENIC PACKAGING

Key to the insertion of superconducting microwave circuits into electronic systems is the integration of the HTS components with a cryogenic refrigerator and its associated control electronics. Clearly, for HTS technology to be ultimately successful, the user must be rendered able to ignore the fact that cryogenics are used at all, by providing long-lifetime cryocoolers and optimally small cryogenic packages with standard envelop characteristics and interfaces (e.g., 19 in rack mounts and back-plane blind-mate connectors).

Many important considerations enter into the design of a cryogenic package suitable for a microwave HTS subsystem. Figure 15 is a schematic representation of this package, showing its main elements and the various heat inputs that must be considered for an appropriate thermal design. Ref. 41 provides specific details on the cryogenic package for a communications filter subsystem.

The choice of a cryocooler will depend on the system and the cooling requirements. An airborne military application may require the use of a small Stirling-cycle cooler because of volume restrictions. On the other hand, a communications ground station in a remote location that needs to operate unattended for a long time may require a larger, more reliable refrigerator of the Gifford–McMahon type. Cooling requirements are imposed by the component or subsystem to be cooled and will determine the amount of cooling power required at the operating temperature. Typical sample system and cooling requirements and some comments as to their significance are given in Tables 4 and 5, respectively.

Table 6. Some Cryogenic Refrigerator Types Likely to Be Used in HTS Technology

Cooler Type	Heat-Lift Range Available at 80 K	Comments
Split Stirling	0.5–3 W	Available from many manufacturers; used primarily in the tactical military infrared detector industry. Has a cold head separated from a compressor by a metallic transfer line up to 15 cm long
Integral Stirling	0.5–5 W	Also used in infrared detectors; at least one version is being used in an HTS development prototype. The compressor and cold finger are integrated into one unit
Gifford–McMahon	2–>200 W	Widely used in the support of vacuum systems for semiconductor industry; highly reliable and versatile. The compressor and cold head are separate units connected by fluid lines that can be several meters long
Throttle-cycle	~4 W	Reliable and low cost. The compressor and cold head are separate units connected by fluid lines that can be several meters long
Joule–Thomson	0.5–2 W	Generally used as an open-cycle cooling system for short tactical missile IR detector applications
Pulse tube	0.5–2 W	Emerging technology, low cold-head vibration and long lifetime potential

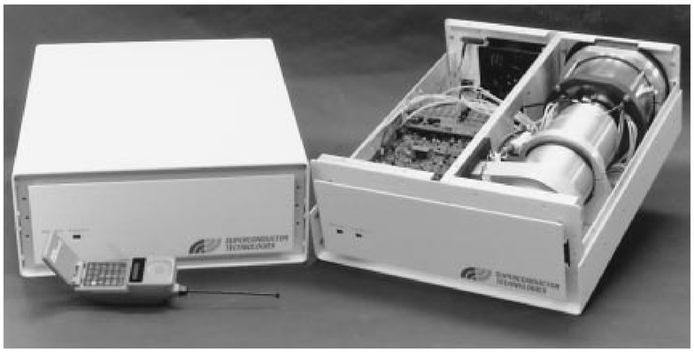

Figure 16. Photograph of a HTS filter assembly for commercial wireless applications (courtesy of Superconductor Technology, Inc.).

Cryocoolers likely to be used in microwave HTS technology will typically have from 1 W to 5 W of cooling capacity. A primary concern systems designers have is the reliability of cryogenic refrigerators, which varies greatly depending on their type and size. Leveraging developments in other fields, such as infrared detectors, the reliability of small, military tactical cryocoolers has steadily increased in recent years, with some manufacturers claiming up to 20,000 h of mean-time to failure (MTTF). On the other hand, larger laboratory or industrial units and specialized coolers for aerospace applications operate for 5 years to 10 years and require minimal servicing. Table 6 lists some of the cryocooler types of interest. The intent here is not to be all-inclusive but to provide a basic reference to the type of coolers most likely to be employed in HTS microwave technology. Reference 56 as a good source of the latest developments in cryocooler technology. Figure 16 is a photograph of a commercial HTS filter subsystem, showing the cryocooler and associated electronics in their open package.

CONCLUSION

High-temperature superconductor microwave technology offers unique advantages derived from the low microwave loss of HTS materials and the inherent low thermal noise in cryogenically cooled components. The main applications to date are related to increased microwave receiver sensitivity, and this is most likely to have an impact on wireless military and commercial communications systems. The reason is that receiver sensitivity and dynamic range must be preserved in the presence of a large number of spurious signals which, if unfiltered, degrade receiver performance. Generation of clean transmitted signals requires filtering in the transmitter and this, coupled with the need to reject unwanted high-power signals at the receiver, has spurred work on high-power handling in HTS filters. Great interest in the United States and abroad exists in the wireless commercial communications market and several companies are testing base-station receiver front-ends consisting of cryogenically-cooled filter-LNA subassemblies.

HTS microwave filters are therefore a promising technology, especially at frequencies below 3 GHz where the loss in conventional microwave materials force high-performance filters to be very large in order to achieve the required low insertion losses and selectivity. Leveraging developments in infrared imaging detector technology and perhaps new developments of cooled semiconductor components for fast computer workstations, cryocooler technology is progressing to the point where long lifetimes and small-size, low-weight coolers are now widely available.

BIBLIOGRAPHY

1. R. S. Withers and R. W. Ralston, Superconductive analog signal processing devices, *Proc. IEEE,* **77**: 1247–1263, 1989. This paper contains many references to earlier work by the authors.
2. P. A. Smith et al., YBCO thick films for high Q resonators, *IEEE Trans. Appl. Supercond.,* **7**: 1763–1765, 1997.
3. D. W. Face et al., Large area $YBa_2Cu_3O_7$ films for high power microwave applications, *IEEE Trans. Appl. Supercond.,* **5**: 1581–1586, 1995.
4. A. Pique et al., Microwave compatible $YBa_2Cu_3O_{7-x}$ films on ferrimagnetic garnet substrates, *Appl. Phys. Lett.,* **67**: 1778–1780, 1995.
5. E. J. Smith, J. Musolf, and E. Soares, Composition controlled MOCVD as a route to high Q HTS thin film devices, *Proc. 3rd Jt. ISTEC/MRS Int. Workshop Supercond.: Suitable Mater. Proces. HTS Appl. Towards Next Decade,* 1997, p. 145.
6. B. Utz et al., Deposition of YBCO and NBCO films on areas of 9 inches in diameter, *IEEE Trans. Appl. Supercond.,* **7**: 1272–1277, 1997.
7. J. W. Ekin, A. J. Panson, and B. A. Blankenship, Method for making low-resistivity contacts to high T_c superconductors, *Appl. Phys. Lett.,* **52**: 331–333, 1988.
8. S. H. Talisa et al., High-temperature superconducting space-qualified multiplexers and delay lines, *IEEE Trans. Microw. Theory Tech.,* **44**: 1229–1239, 1996.
9. R. K. Hoffmann, *Handbook of Microwave Integrated Circuits,* Norwood, MA: Artech House, 1987.
10. G. L. Matthaei, L. Young, and E. M. T. Jones, *Microwave Filters, Impedance-Matching Networks, and Coupling Structures,* Dedham, MA: Artech House, 1980.
11. Z.-Y. Shen, *High-Temperature Superconducting Microwave Circuits,* Norwood, MA: Artech House, 1994.
12. S. Ramo, J. R. Whinnery, and T. Van Duzer, *Fields and Waves in Communication Electronics,* New York: Wiley, 1965.
13. I. Vendik and O. Vendik, in E. Kollberg (ed.), *High Temperature Superconductor Devices for Microwave Signal Processing,* St.-Petersburg, Russia: Scladen, 1997, 3 parts.
14. K. R. Carroll, J. M. Pond, and E J. Cukauskas, Superconducting kinetic-inductance microwave filters, *IEEE Trans. Appl. Supercond.,* **3**: 8–16, 1993.
15. Unpublished data obtained jointly by Northrop Grumman, NASA Lewis Research Center and Superconductor Technology, Inc.
16. W. W. Mumford and E. H. Scheibe, *Noise Performance Factors in Communication Systems,* Dedham, MA: Horizon House-Microwave, 1968, UMI Out-of-Print Books on Demand.
17. S. H. Talisa et al., Dynamic range considerations for high-temperature superconducting filter applications to receiver front-ends, *IEEE MTT-S Int. Microw. Symp. Dig.,* 1994, pp. 997–1000.
18. J. B.-Y. Tsui, *Microwave Receivers with Electronic Warfare Applications,* Malabar, FL: Krieger, 1992.
19. G. Koepf, Superconductors improve coverage in wireless networks, *Microw. RF,* **37** (4): 63–74, 1998.
20. D. E. Oates et al., Nonlinear surface resistance in $YBa_2Cu_3O_{7-x}$ thin films, *IEEE Trans. Appl. Supercond.,* **3**: 1114–1119, 1993.

21. C. Wilker et al., Nonlinear effects in high-temperature superconductors: 3rd order intercept from harmonic generation, *IEEE Trans. Appl. Supercond.,* **5**: 1665–1670, 1995.
22. M. Golosovsky, Physical mechanisms causing nonlinear microwave losses in high-T_c superconductors, *8th Workshop RF Supercond.,* Abano Terme, Italy, 1997, Invited Paper.
23. S. Sridhar, Non-linear microwave response of superconductors and ac response of the critical state, *Appl. Phys. Lett.,* **65**: 1054–1056, 1994.
24. J. H. Oates et al., A nonlinear transmission line model for superconducting stripline resonators, *IEEE Trans. Appl. Supercond.,* **7**: 17–22, 1993.
25. D. E. Oates et al., Microwave power dependence of $YBa_2Cu_3O_7$ thin-film Josephson edge junctions, *Appl. Phys. Lett.,* **68**: 705–707, 1996.
26. I. Vendik and O. Vendik, *High Temperature Superconducting Devices for Microwave Signal Processing,* St. Petersburg, Russia: Skladen, 1997, Part 2, Chap. 7.
27. B. S. Karasik et al., Subnanosecond switching of YBaCuO films between superconducting and normal states induced by current pulse, *J. Appl. Phys.,* **77**: 4064–4070, 1995.
28. I. Vendik et al., The superconducting microwave devices based on S-N transition in HTS films, *27th Eur. Microw. Conf. Proc.,* 1997, pp. 909–914.
29. Z.-Y. Shen et al., Power handling capability improvement of high-temperature superconducting microwave circuits, *IEEE Trans. Appl. Supercond.,* **7**: 2446–2453, 1997.
30. Z. Ma et al., RF power dependence study of large area YBCO thin films, *IEEE Trans. Appl. Supercond.,* **7**: 1911–1916, 1997.
31. T. Dahm and D. J. Scalapino, Theory of intermodulation in a superconducting microstrip resonator, *J. Appl. Phys.,* **81**: 2002–2009, 1997.
32. O. G. Vendik, I. B. Vendik, and T. B. Samoilova, Nonlinearity of superconducting transmission line and microstrip resonator, *IEEE Trans. Microw. Theory Tech.,* **45**: 173–178, 1997.
33. S. H. Talisa et al., Low- and high-temprature superconducting microwave filters, *IEEE Trans. Microw. Theory Tech.,* **39**: 1448–1454, 1991.
34. W. G. Lyons et al., High-T_c superconductive microwave filters, *IEEE Trans. Magn.,* **27**: 2537–2539, 1991.
35. W. G. Lyons and L. H. Lee, Accuracy issues and design techniques for superconducting microwave filters, *Comput.-Aided Des. Supercond. Microw. Components Workshop, IEEE Int. Microw. Symp.,* 1994. The authors are with Lincoln Laboratory, Massachusetts Institute of Technology.
36. D. Zhang et al., Compact forward-coupled superconducting microstrip filters for cellular communications, *IEEE Trans. Appl. Supercond.,* **5**: 2656–2659, 1995.
37. G. L. Matthaei and G. L. Hey-Shipton, Novel staggered resonator array superconducting 2.3-GHz bandpass filter, *IEEE Trans. Microw. Theory Tech.,* **41**: 2345–2352, 1993.
38. D. G. Swanson, R. Forse, and B. J. L. Nilsson, A 10 GHz thin film lumped element high temperature superconductor filter, *IEEE MTT-S Int. Microw. Symp. Dig.,* 1992, pp. 1191–1193.
39. D. G. Swanson and R. Forse, An HTS end-coupled CPW filter at 35 GHz, *IEEE MTT-S Int. Microw. Symp. Dig.,* 1994, pp. 199–202.
40. A. Vogt and W. Jutzi, An HTS narrow bandwidth coplanar shunt inductively coupled microwave bandpass filter on $LaAlO_3$, *IEEE Trans. Microw. Theory Tech.,* **45**: 493–497, 1997.
41. M. J. Scharen et al., Filter subsystems for wireless communications, *IEEE Trans. Appl. Supercond.,* **7**: 3744–3749, 1997.
42. R. R. Mansour et al., Design considerations of superconductive input multiplexers for satellite applications, *IEEE Trans. Microw. Theory Tech.,* **44**: 1213–1228, 1996.
43. C. Rauscher, J. M. Pond, and G. B. Tait, Cryogenic microwave channelized receiver, *IEEE Trans. Microw. Theory Tech.,* **44**: 1240–1247, 1996.
44. S. J. Fiedziuszko et al., Low loss multiplexers with planar dual mode HTS resonators, *IEEE Trans. Microw. Theory Tech.,* **44**: 1248–1257, 1996.
45. N. O. Fenzi et al., An optically switched bank of HTS bandstop filters, *IEEE MTT-S Int. Microw. Symp. Dig.,* 1994, pp. 195–198.
46. S. H. Talisa et al., High-temperature superconducting four-channel filterbanks, *IEEE Trans. Appl. Supercond.,* **5**: 2079–2082, 1995.
47. T. G. Kawecki et al., The high temperature superconductivity space experiment (HTSSE-II) design, *IEEE Trans. Microw. Theory Tech.,* **44**: 1198–1212, 1996.
48. G.-C. Liang et al., High-temperature superconducting microstrip filters with high power handling capability, *IEEE MTT-S Int. Microw. Symp. Dig.,* 1995, pp. 191–194.
49. H. Chaloupka et al., Superconducting planar disk resonators and filters with high power handling capability, *Electron. Lett.,* **32**: 1735–1736, 1996.
50. S. Kolesov et al., Planar HTS structures for high-power applications in communication systems, *J. Supercond.,* **10**: 179–187, 1997.
51. W. G. Lyons et al., High temperature superconductive wideband compressive receivers, *IEEE Trans. Microw. Theory Tech.,* **44**: 1258–1278, 1996.
52. G. C. Liang et al., Space-qualified superconductive digital instantaneous frequency-measurement subsystem, *IEEE Trans. Microw. Theory Tech.,* **44**: 1289–1299, 1996.
53. N. Fenzi et al., Development of high temperature superconducting 100 nanosecond delay line, *SPIE Proc.,* **2156**: 143–151, 1994.
54. S. H. Talisa et al., High-temperature superconducting wide band delay lines, *IEEE Trans. Appl. Supercond.,* **5**: 2291–2294, 1995.
55. M. Biehl et al., A 4-bit instantaneous frequency meter at 10 GHz with coplanar YBCO delay lines, *IEEE Trans. Appl. Supercond.,* **5**: 2279–2282, 1995.
56. R. G. Ross, Jr. (ed.), *Cryocoolers 9, A Publication of the International Cryocooler Conference,* New York: Plenum, 1997.

SALVADOR H. TALISA
Northrop Grumman Corporation

SUPERCONDUCTING HIGH-ENERGY PARTICLE DETECTOR MAGNETS. See HIGH-ENERGY PHYSICS PARTICLE DETECTOR MAGNETS.